Single-channel Properties of Recombinant Acid-sensitive Ion Channels Formed by the Subunits ASIC2 and ASIC3 from Dorsal Root Ganglion Neurons Expressed in *Xenopus* Oocytes

Ping Zhang and Cecilia M. Canessa

From the Department of Cellular and Molecular Physiology, Yale University School of Medicine, New Haven, Connecticut 06520

ABSTRACT The acid-sensitive ion channels known as ASIC are gated by external protons. A set of these channels is expressed in dorsal root ganglion neurons where they may participate in the transduction of mechanical and nociceptive stimuli. Here, we have examined the single-channel properties of channels formed by the subunits ASIC2 and ASIC3 expressed in *Xenopus* oocytes using outside-out patches. The mean single-channel current-voltage relationship is linear with a slope conductance of 18 pS between −80 and −40 mV in 150 mM Na^+ outside and 150 mM K^+ inside the patch pipet. The selectivity for monovalent cations has the sequence $Na^+ > Li^+ > K^+$. Divalent cations such as Ca^{2+} do not permeate, but instead block the channel when applied to the extracellular side. External protons increase the probability of channels being open to a maximum of 0.8 with an EC_{50} of 16 ± 4 μM and a Hill coefficient of 2.7 ± 0.3, whereas the mean single-channel current amplitude is independent of external pH. Analysis of the kinetics of single channels indicates the presence of at least four modes of activity (Mod1 to Mod4) in addition to an inactivated state. Three of the modes exhibit distinct kinetics, and can be unambiguously identified on the basis of open probability ($P_{oMod1} = 0.5 \pm 0.05$; $P_{oMod2} > 0.9 \pm 0.05$; $P_{oMod3} < 0.1$). Mode 4, which has a P_o in the range of 0.5–0.8, may constitute a distinct mode or alternatively, it represents transitions between the other three modes of activity. Increasing $[H^+]_o$ increases the frequency of entering the modes with high P_o (modes 1, 2, and 4) and the time the channel spends in the modes with high activity.

KEY WORDS: protons • pH • degenerins • nociception • mechanoreceptor

INTRODUCTION

The acid-sensitive ion channels (ASIC)[1] are a family of proteins closely related in amino acid sequence and structure to the epithelial sodium channel (ENaC) and to the degenerins from *Caenorhabditis elegans* (mec-4, mec-10, and deg-1). They constitute a class of ion channels known as the DEG/ENaC superfamily (Corey and Garcia-Añoveros, 1996; Fyfe et al., 1998). So far, six ASIC cDNAs corresponding to four genes have been cloned from mammalian organisms: ASIC1 (Garcia-Añoveros et al., 1997; Waldmann et al., 1997a), ASIC2 (or BNC; Price et al., 1996; Garcia-Añoveros et al., 1997), ASIC3 (or DRASIC; Waldmann et al., 1997a), and ASIC4 (or SPASIC; Akopian et al., 2000; Gründer et al., 2000). In addition, a spliced form of ASIC2, named ASIC2b (Lingueglia et al., 1997), and of ASIC1, named ASICβ (Chen et al., 1998), have been identified. All of them are expressed primarily in neurons from either the central or peripheral nervous systems. Experiments of in situ hybridization indicate that many neurons coexpress more than one of the ASIC proteins.

Characteristic of ASIC is that external protons ($[H^+]_o$) activate the channels (Waldmann et al., 1999). Expression of any ASIC in *Xenopus* oocytes or in mammalian cells induces an acid-activated conductance whose properties vary according to the specific combination of subunits being expressed. The most significant functional differences among these channels are the sensitivity to external protons and the kinetics of activation and inactivation (Waldmann et al., 1999). For instance, channels formed only by ASIC1 inactivate in a few seconds, whereas channels formed by ASIC3 produce sustained currents (Waldmann et al., 1997b).

The physiological roles and functional pathways that depend on ASIC have not been well defined. However, selective expression of some of these proteins in dorsal root ganglion (DRG) neurons has suggested that they may participate in nociception and/or mechanoperception (Waldmann et al., 1997a; Chen et al., 1998). DRG neurons exhibit various acid-sensitive cation conductances (Akaike et al., 1990; Bevan and Yeats, 1991), some of which have been implicated in nociception induced by tissue acidification, as occurs during inflammation or injury. It is now clear that the vallinoid receptor (VR-1), a channel gated by heat and also protons, underlies most

Address correspondence to Cecilia M. Canessa, 333 Cedar Street, New Haven, CT 06520-8026. Fax: (203) 785-4951; E-mail: cecilia.canessa@yale.edu

[1]*Abbreviations used in this paper:* ASIC, acid-sensitive ion channels; DRG, dorsal root ganglion; ENaC, epithelial sodium channel; P_o, open probability.

of the acid-activated currents in a population of small neurons from DRG (Tominaga et al., 1998). However, in a knockout mouse with inactivation of the VR-1 gene, DRG neurons continue to express acid-activated currents, indicating that other proton-gated channels are still functional (Caterina et al., 2000).

On the other hand, the idea that ASIC may represent a mechanoreceptor arose from the homology of these channels with the degenerins. The degenerins were initially identified by screening animals for deficits in light touch (Driscoll and Chalfie, 1991; Huang and Chalfie, 1994). Mutations that activated the proteins induced degeneration of a set of neurons involved in touch perception and inactivating mutations rendered the animals touch-insensitive. These results suggested that the degenerins were involved in mechanotransduction in *C. elegans*. Recently, the mouse ASIC2 gene was disrupted. The phenotype of the knockout mouse was unremarkable, but careful examination of fibers innervating the skin revealed that the low threshold, rapidly adapting and, to a lesser degree, the slowly adapting mechanoreceptors showed a reduced discharge frequency upon stimulation when compared with wild-type animals (Price et al., 2000).

Several lines of evidence suggest that these two proteins form heteromeric channels. When the two subunits are coexpressed in heterologous systems, such as the oocyte, they induce currents larger in magnitude and with different properties than if any of the two subunits is expressed alone. Biochemical association of ASIC2 and ASIC3 has been shown in vitro by coimmunoprecipitation of the two proteins tagged with six-His and FLAG epitopes in oocytes (Babinski et al., 2000). Finally, in recent experiments using specific antibodies against ASIC2 and ASIC3, we have demonstrated that ASIC2 and ASIC3 are coexpressed in the same population of cells from dorsal root ganglia (Alvarez de la Rosa, D., P. Zhang, D. Shao, F. White, and C. Canessa, manuscript in preparation). Together, the evidence strongly supports the existence of ASIC2-3 channels in vivo.

The purpose of this study is to describe the effects of external protons and the properties of unitary currents of channels formed by the association of ASIC2 and ASIC3 to understand their functional role in sensory neurons.

MATERIALS AND METHODS

Expression of Channels in Xenopus Oocytes

Channels were expressed in stage V and VI *Xenopus laevis* oocytes injected with 2 ng of cRNA from each ASIC2 and ASIC3. cRNAs were synthesized with T7 RNA polymerase from linearized plasmids containing the full-length cDNAs of ASIC2 and ASIC3 cloned by reverse transcriptase–PCR from rat mRNA. Oocytes were incubated at 19°C for 2–5 d before making recordings. Before patching, oocytes were placed in an hyperosmotic solution for several minutes, and the vitelline membrane was removed manually with fine forceps.

Single-channel Recording

Currents were recorded from ASIC2-3 channels using the outside-out configuration of the patch-clamp technique. Experiments were performed on patches containing single channels unless indicated in the text. We determined the number of channels in the patch by performing recordings of several minute durations and counting the number of transition levels observed in the patch. We also applied a solution of pH_o 4.0 to the outside-out patch, which is expected to maximally activate the channels present in the patch. Patches containing multiple channels were discarded from kinetics analysis.

Pipets were pulled from borosilicate glass (LG16; Dagan Corporation) using a micropipet puller (model PP-83 Narishige; Scientific Instrument Lab), fire-polished to a final tip diameter of 1 μm, and coated with Sylgard. When pipets were filled with solutions, they had resistances of 10–20 MΩ. Single-channel currents were recorded with an Axopatch-200B amplifier (Axon Instruments) using a TL-1 interface and pClamp6.0 software both from Axon Instruments. The data were filtered at 2–5 kHz, digitized at a sampling interval of 40 μs, and stored on a computer hard disk for analysis. For display, data were filtered with a digital Gaussian filter to 1 kHz.

All experiments were carried out at room temperature. The composition of solutions is given in millimolars. Incubation solution for oocytes: 96 NaCl, 2 KCl, 1 $MgCl_2$, and 5 HEPES, adjusted to pH 7.4. Hyperosmotic solution to remove the vitelline membrane: 220 NMDG, 220 aspartic acid, 2 $MgCl_2$, 10 EGTA, and 10 HEPES, adjusted to pH 7.4 with KOH. Solution in the recording microchamber (extracellular): 150 NaCl, 1.8 $CaCl_2$, and 10 Mes-Tris, adjusted to pH 7.4. For activation of ASIC channels, outside-out patches were perfused with solutions of composition identical to the extracellular solution but buffered to a lower pH, either 6.0, 5.0, 4.0, or as indicated in the experiment. To examine the selectivity of the channel for various cations, we replaced 150 NaCl with 150 LiCl or 150 KCl in the perfusion solutions, which were buffered to pH 4.0 for maximal activation of channels. Pipet solution (intracellular): 150 KCl, 5 EDTA, and 5 HEPES, adjusted to pH 7.4 with KOH.

Application of Solutions of Low pH to Outside-out Patches

The starting solution facing the tip of the pipet corresponding to the bath solution was always pH 7.4. Channels were activated by applying solutions of low pH_o to outside-out patches using a solution delivery device that achieves complete solution changes within 20 ms (model SF-77B perfusion fast-step; Warner Instrument Corp.). Typically, three solutions were continuously flowing from three squared glass tubes (ID 0.7 mm). The patch pipet was initially positioned in front of the middle tube, which delivered a solution of pH_o 7.4, and then moved with a voltage-command step to either of the other tubes, which delivered test solutions of lower pH: 6.0, 5.0, or 4.0, or as indicated in the particular experiment.

Whole-cell Recordings

For two-microelectrode recordings, current and voltage electrodes were pulled from borosilicate glass and filled with 3 M KCl. The resistance was kept in the range of 0.5–1 MΩ. Oocytes were clamped at −60 mV and current-voltage relations were generated by changing the membrane potential from −150 or −100 to 50 or 100 mV in 10-mV incremental steps of 200 ms duration. Currents were recorded with an oocyte clamp (model OC-725B; Warner Instrument Corp.), digitized with a sampling rate of 100

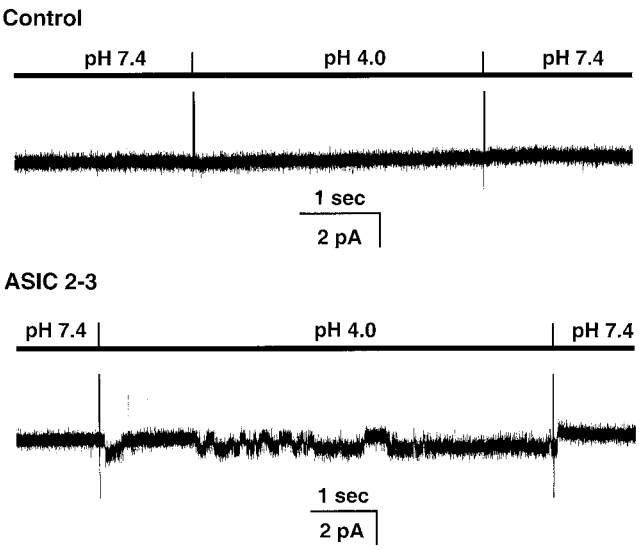

FIGURE 1. Response of outside-out patches to a pH_o 4.0 solution from control and injected oocytes with ASIC2-3 cRNAs. External protons evoke inward currents (downward deflections) only in oocytes injected with ASIC2-3. In none of the ~40 control oocytes we observed acid-activated channels. The bars above the traces indicate the applied pH_o. Membrane potential was −20 mV. The outside solution contained 150 mM NaCl, and the pipet solution contained 150 mM KCl.

Hz (model ITC-16; HEKA), and the data were stored on the hard disk of a PC. The oocyte chamber (volume of 300 μl) was continuously perfused at 1–2 ml/min. The composition of the standard bath solution contained (in mM) 100 NaCl, 2 KCl, and 1 $CaCl_2$; bath solution without Na^+ contained (in mM) 50 $CaCl_2$ and 2 KCl; and bath solution with Na^+ and Ca^{2+} contained (in mM) 100 NaCl, 2 KCl, and 50 $CaCl_2$. All solutions were buffered with 10 HEPES and 10 MES, and the pH was adjusted to 7.4 or 4.0. Sorbitol was added to keep osmolality at 250 mOsm.

Data Analysis

Amplitude histograms were binned into equally spaced bins and fitted with the sum of two Gaussian components, using the method of least-squares minimization. Lists of the duration of single-channel events were generated using the half-amplitude threshold criterion. Histograms of the distributions of the open and closed dwell times were plotted as the logarithm of the dwell-time duration, with a square root transformation of the ordinate, and fitted with the sum of several exponential components using the maximal likelihood method of least-squares minimization. Data points represent the mean of at least three independent measurements ±SD.

Definition of Modes of Activity. Only patches containing single channels were examined. Visual inspection of these records revealed that the kinetics of ASIC2-3 channels are not stationary but exhibit modes of activity. This impression was confirmed by analysis of P_o with stability plots. We selected, from 3 to 5 min of continuous recording from the same patch, segments with low P_o (<0.1), intermediate P_o (~0.5), and high P_o (>0.9). Selected segments from each of the three groups were analyzed together as a continuous record and reexamined for kinetics and P_o. Misclassified segments were removed from further analysis. Data from the three groups (modes 1, 2, and 3) were used for generating histograms of open and closed events. The rest of the records, comprising 30–40% of channel activity, were considered as a mixture of modes (mode 4) or as unclassified.

RESULTS

Identification of Single ASIC2-3 Channels in Oocytes

Exposure of outside-out patches to solutions of low pH_o evoked single-channel activity in membranes from oocytes injected with ASIC2-3 cRNAs but not in uninjected oocytes. On average, the frequency of detecting acid-activated channels in injected oocytes was 7 out of 10 patches, whereas control oocytes did not express acid-activated channels. Fig. 1 shows representative examples of unitary currents elicited by perfusion with an external solution buffered at pH_o 4.0. The spikes in the recording indicate the change of solutions. No channel activity is detected at pH_o 7.4; when the pH_o is changed to 4.0, a channel opens (downward deflections) and it closes after returning to pH_o 7.4. When multichannel patches were exposed to several sequential changes of pH_o, the number of activated channels progressively decreased. This effect was more pronounced at high $[H^+]_o$.

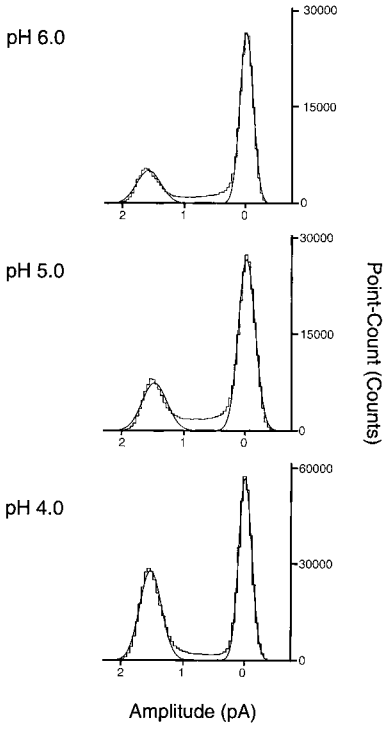

FIGURE 2. All-points amplitude histograms of single-channel currents elicited by solutions of pH_o 6.0, 5.0, and 4.0 recorded from outside-out patches at −80 mV and with 150 mM Na^+ in the bath and 150 mM K^+ in the pipet. The distributions were fitted by the sum of two Gaussian components (continuous lines). The mean amplitude of the open state is −1.8 ± 0.01 pA for the three different pH_o solutions. The areas under the curves are as follows: 0.2 and 0.8 at pH_o 6.0; 0.28 and 0.72 at pH_o 5.0; and 0.45 and 0.55 at pH_o 4.0. Since the average P_o at pH_o 6.0 is low, we chose a segment of high activity to obtain a significant number of points on the open state.

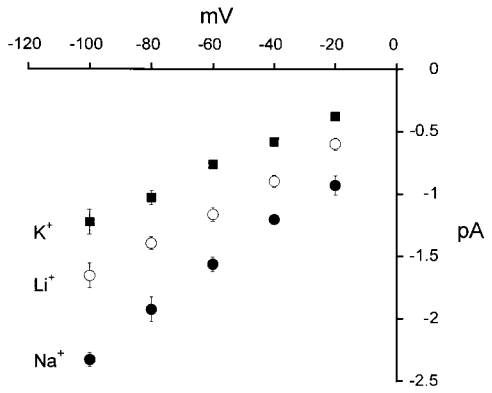

FIGURE 3. Current-voltage relationships of single-channel currents. Mean I-V relationship of single-channel currents from outside-out patches activated by pH_o of 4.0 recorded at membrane potentials from −100 to −20 mV. External solution contained 150 mM of Na^+, Li^+, or K^+, and internal solution contained 150 mM K^+. Data points represent the mean of at least three independent measurements. The error bars indicate ±SD.

Conductance and Selectivity of ASIC2-3 Channels

Fig. 2 shows all-points amplitude histograms of currents evoked by pH_o 6.0, 5.0, and 4.0 recorded with 150 mM Na^+ in the external solution and 150 mM K^+ in the pipet. At −80 mV of membrane potential, the amplitude of the unitary current is −1.8 ± 0.04 pA with solutions of pH_o 6.0, 5.0, and 4.0. The shoulder between the peaks and the small differences in conductance at the various pH_o are mainly due to short events that do not reach full amplitude.

Current-voltage relationships from unitary currents were obtained at pH_o 4.0 in the presence of 150 mM external Na^+, Li^+, or K^+ and 150 mM internal K^+ (Fig. 3). The amplitude of the unitary currents is larger with Na^+ than with Li^+, and larger with Li^+ than with K^+ outside. Under these experimental conditions, the slope conductance calculated between −80 and −40 mV is 18 pS for Na^+, 12 pS for Li^+, and 11 pS for K^+.

In symmetric K^+, the I-V curve is linear over the range of voltages from −100 to −20 mV, indicating that the unitary conductance of ASIC2-3 is not voltage dependent. With Li^+ or Na^+ outside and K^+ inside, the I-V curves show slight inward rectification as expected from the higher conductance of these two ions over K^+.

Effect of Ca^{2+} Ions on the Activity of ASIC2-3

From previous studies it has been reported that some of the ASIC channels are permeable to divalent cations; specifically, that ASIC1 conducts Ca^{2+} (Waldmann et al., 1997a). We examined whether channels formed by ASIC2 and ASIC3 are permeable to Ca^{2+} by replacing all monovalent cations from the external patch solution with 75 mM Ca^{2+}. This solution buffered to pH_o 4.0 did not elicit inward currents in patches from oocytes injected with ASIC2-3, indicating that the permeability to Ca^{2+} is very small or absent. However, very small unitary currents cannot be detected with the patch-clamp technique. Therefore, we examined whole-cell currents from oocytes with solutions containing either 100 mM Na^+ or 50 mM Ca^{2+} as the only external cations. The concentration of Cl^- in both solutions was the same and the osmolarity was adjusted to 250 mOsm with sorbitol. Fig. 4 A shows that a bathing solution containing 100 mM Na^+ buffered at pH_o 4.0 elicits large inward currents that revert at 40 mV. Replacement of all external Na^+ by 50 mM Ca^{2+} eliminates the inward current

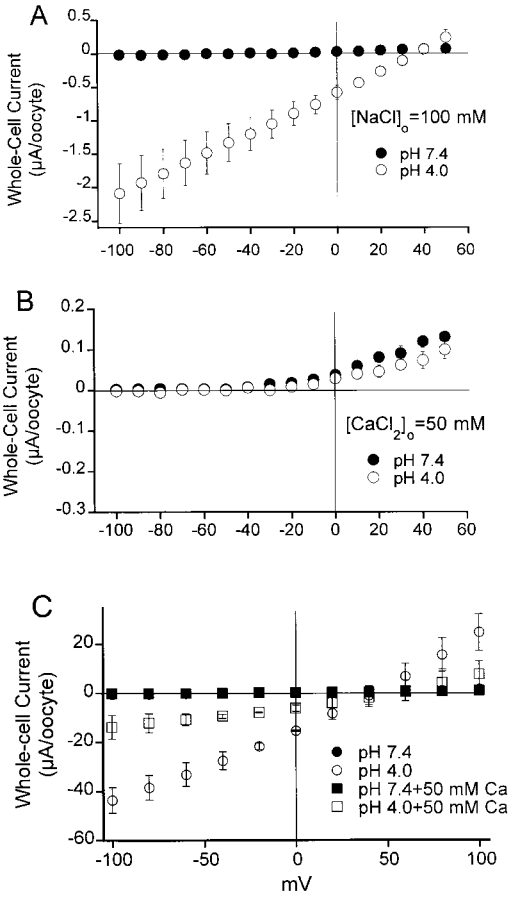

FIGURE 4. Mean I-V relationships of whole-cell currents from oocytes expressing ASIC2-3 measured with a two-electrode voltage clamp. (A) The external solution contains 100 mM NaCl buffered at pH 7.4 or 4.0; voltage range of membrane potential was −100 to 50 mV. (B) The external solution contains 50 mM $CaCl_2$ without Na^+, buffered to pH 7.4 or 4.0; voltage range of membrane potential was −100 to 50 mV. Notice the change in the scale of the vertical axis. Inward and outward currents become very small in the absence of Na^+, and the symbols representing the currents at pH_o 7.4 and 4.0 are almost superimposed. (C) The external solution contains 100 mM NaCl and 50 mM Ca_2Cl buffered at pH 7.4 or 4.0. At pH_o 7.4, no currents are detected; black squares and circles are superimposed. To better observe the effect of Ca^{2+} on both inward and outward currents, the voltage range of the membrane potential was expanded from −150 to 100 mV. Each data point is the mean of three to four oocytes ±SD.

and displaces the reversal potential to the left (Fig. 4 B). In addition, external Ca^{2+} also diminishes the outward current. Notice that the scale of the vertical axis in Fig. 4 B has been expanded to better appreciate the small outward currents. However, removal of external Na^+ should not affect the outward current because it is predominantly carried by the exit of intracellular K^+ ions through ASIC2-3 activated by low pH_o. This result suggests that Ca^{2+} may block ASIC2-3.

To examine the possibility that Ca^{2+} blocks Na^+ currents conducted by ASIC2-3, we compared whole-cell I-V relationships in the presence of 100 mM Na^+ as the current carrier with and without 50 mM Ca^{2+} in the bath solution (Fig. 4 C, squares and circles, respectively). As before, no currents are detected at pH_o 7.4. The black symbols, representing currents at pH_o 7.4 ± 50 mM Ca^{2+} are superimposed. pH_o 4.0 induces large currents that are partially blocked by 50 mM Ca^{2+} (open symbols), 70% block at −100 mV. Other divalent cations such as Zn^{2+} and Mg^{2+} also block ASIC2-3 channels (data not shown). These experiments, together with the fact that we did not see activation of the very abundant endogenous Ca^{2+}-activated Cl^- channels from oocytes, indicate that ASIC2-3 is not permeable to Ca^{2+}; on the contrary, divalent cations block this channel.

Properties of the Fast and Sustain Components of ASIC2-3 Currents

Whole-cell currents from cells expressing ASIC2-3 exhibit a biphasic behavior (Waldmann et al., 1999; Babinski et al., 2000). The initial phase, referred to as the fast component, immediately follows the change to a low pH_o (Fig. 5 A). The fast current partially inactivates and, according to previous reports, the selectivity for ions, pH_o sensitivity, and amiloride affinity differ from the sustain current. We investigated the mechanism underlying these two components of the macroscopic current of ASIC2-3 by examining the properties of unitary currents immediately after lowering the pH_o from outside-out patches.

The only significant and reproducible finding immediately after changing the pH_o was on the number of active channels. Fig. 5 B shows two such examples. Lowering the pH_o activates two channels, one closes after the first two seconds, whereas the other remains open for the remainder of the recording. This was a frequent finding, and we used it routinely as a test to estimate the total number of channels in the patch. Another feature of the fast component is that it appears only when pH_o is changed from 7.4 to a lower pH_o, but not if the pH_o is sequentially changed. For instance, if the patch pipet is exposed to 7.4 followed by 6.0, 5.0, and 4.0 without returning to pH_o 7.4, the fast component is seen exclusively in the transition from 7.4 to 6.0 but not during the other pH_o changes.

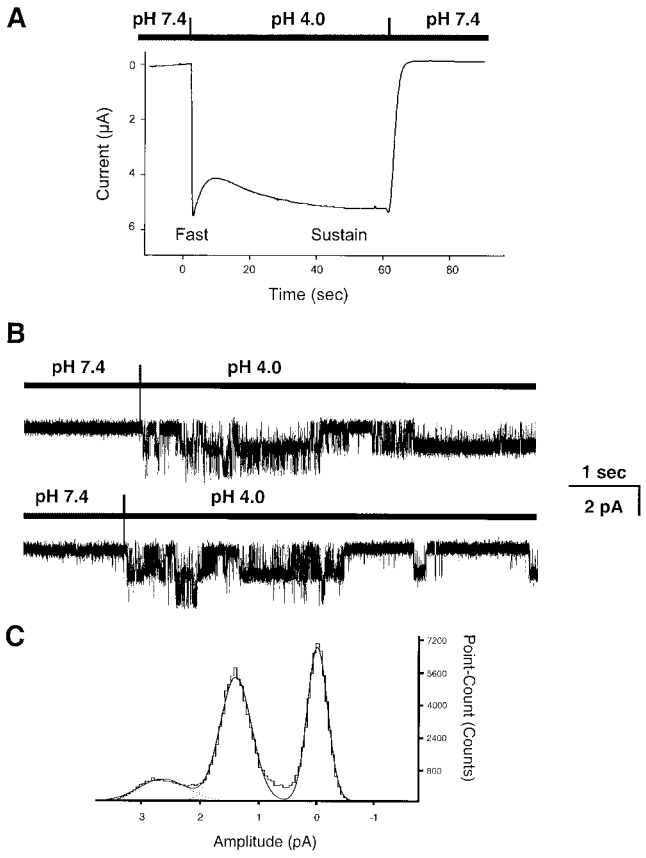

FIGURE 5. Fast and sustain components of ASIC2-3 currents. (A) Whole-cell currents elicited by changing the pH_o from 7.4 to 4.0 in an oocyte expressing ASIC2-3. The initial current (fast component) partially inactivates and it is followed by a sustain component. Holding potential −60 mV; bath solution contains 100 mN Na^+. (B) Outside-out patches showing the activation of channels immediately after changing the external solution from pH_o 7.4 to 4.0. Initially, two channel levels are apparent, but after 2.5 s, one of the channels closes. Holding potential −40 mV; outside solution contains 150 mM Na^+, and pipet solution contains 150 K^+. (C) All-points amplitude histogram from patches showed in B. The distributions were fitted by the sum of three Gaussian components (continuous lines). The mean amplitudes of the open states were −1.3 ± 0.2 pA and −2.6 ± 0.3 for one and two open levels, respectively.

The amplitude of the unitary currents was identical in the initial and late phases (1.3 ± 0.2 pA) as shown by the all-points histogram in Fig. 5 C. In addition, IV curves generated with various ions substitutions during the sustained phase showed that this component of the current has selectivity $Na^+ > K^+ > Li^+$. Together, the results indicate that the fast and sustain components are produced by channels with the same conductance and selectivity. The difference seems to be on the kinetic state of the channels. The fast component is generated by a population of channels that soon after activation enter a long lasting–inactivated state and remain inactive until the pH_o returns to 7.4.

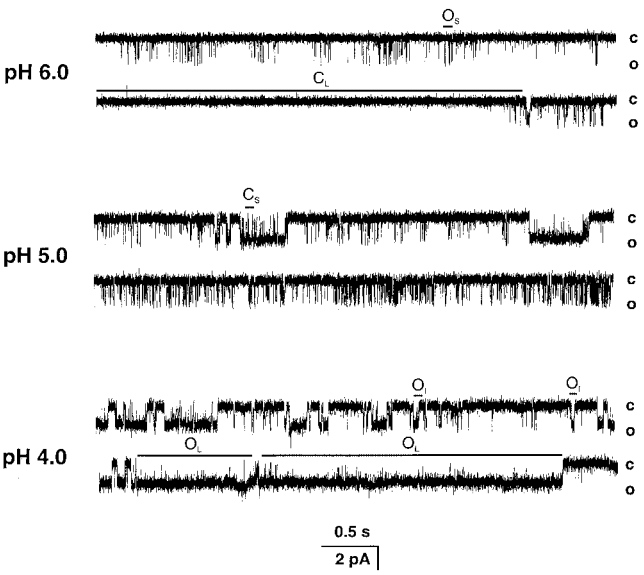

FIGURE 6. Representative examples of outside-out patches containing single ASIC2-3 channels activated by increasing concentrations of external protons, pH_o 6.0, 5.0, and 4.0. Activity of the channel and P_o increase with increasing $[H^+]_o$. At pH_o 6.0, the openings are short and are separated by closed events of variable duration, some of which last several hundred milliseconds. At pH_o 5.0, the short openings increase in frequency and longer openings are apparent. At pH_o 4.0, there is a further increase in P_o due to long openings. The closed and open levels are indicated on the right side. O_S, O_I, and O_L indicate short, intermediate and long open states, respectively. C_S and C_L indicate short and long closed states, respectively. Bath solution contained 150 mM Na^+, and pipet solution contained 140 mM K^+. Membrane potential was held at −60 mV. The data were recorded at 5 kHz and filtered at 1 kHz for display. The bars on the bottom indicate the time and amplitude scales in pA and seconds, respectively.

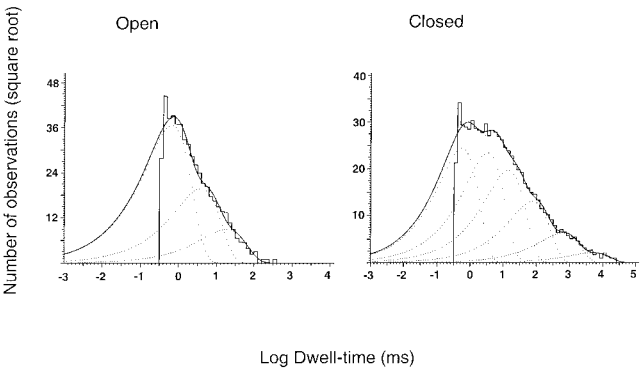

FIGURE 7. Dwell-time histograms of open and closed events collected from three outside-out patches activated with pH_o 5.0. Lines represent the fit of the data of open events with three exponentials. Mean time constant (relative area shown in parentheses) are as follows: 0.66 ms (0.74), 3.9 ms (0.21), and 19 ms (0.05). The closed events were fitted with the following six exponential components: 0.55 ms (0.34), 3.3 ms (0.31), 14 ms (0.21), 75 ms (0.08), 606 ms (0.04), and 4880 ms (0.02).

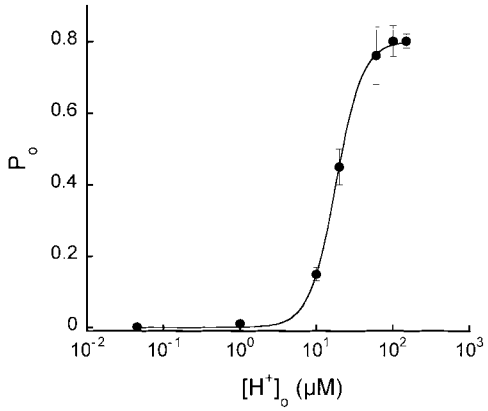

FIGURE 8. External proton dose–response curve. Open probability of ASIC2-3 was plotted for each increment of $[H^+]_o$. Fit of the data to the Hill equation is shown the in solid line. The calculated values were as follows: EC_{50} = 16 μM, Hill coefficient = 2.7, and maximum P_o = 0.8. Symbols represent the mean P_o obtained from at least 10,000 open and closed events. For some of the points, two to three patches activated by the same pH_o were combined to have sufficient number of events for the analysis.

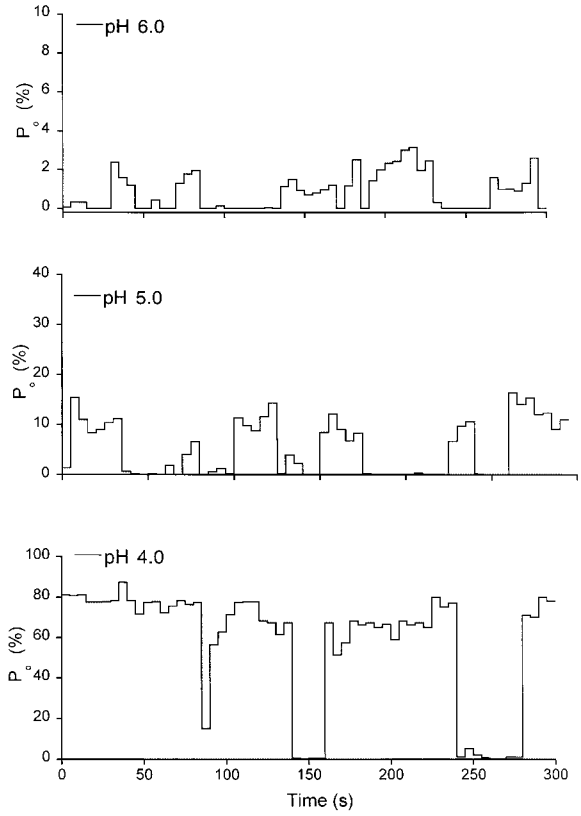

FIGURE 9. Variations of the open probability of ASIC2-3 channels over time. We selected patches containing single channels that lasted for 5 min or longer of continuous recording after activation by solutions of pH_o 6.0, 5.0, and 4.0. The P_o was averaged each 5 s and plotted over 300 s.

Relationship of Channel Activity and pH_o

The activity of ASIC2-3 increases with increasing concentrations of external protons; the effect is seen within the range of pH_o from 6.4 to 4.0. Lowering the pH_o below 4.0 does not induce a further increase in activity.

Fig. 6 shows representative traces of outside-out patches containing single channels activated by pH_o 6.0, 5.0, and 4.0. At pH_o 6.0, the open probability (P_o) is low; in the 20-s recording shown in the top panel, the average P_o is 0.03. Most of the channel openings are of short duration (downward deflections indicated by O_S), and they occur mostly in clusters. The periods of activity are separated by closures of different duration, some of which last several seconds (C_L). Stretches with few short openings where the P_o approaches the zero value are common at pH_o 6.0. At pH_o 5.0, the channel is more active with an average P_o of 0.25. The short openings appear with higher frequency and, in addition, openings of intermediate and long duration (O_I and O_L) are apparent. At pH_o 4.0, there is a further increase in P_o to 0.69 due to more frequent and longer openings.

The number of apparent open and closed states was determined from the distributions of open and closed dwell times from patches containing single channels. To ascertain the number of channels in the patch, we first activated the maximal number of channels by exposing it to pH_o 4.0. Patches that showed more than one current level at any time during the recording were discarded from kinetics analysis. Fig. 7 shows the histograms of open and closed events at pH_o 5.0. Three exponential components were required to describe the distribution of observed open events, suggesting that channels adopt at least three open states. The observed mean channel open times of the three distributions (mean time constant followed by relative area in parentheses) are as follows: 0.66 ms (0.74) for the short openings, 3.9 ms (0.21) for the intermediate openings, and 19 ms (0.05) for the long openings. Six exponential components were required to fit the distributions of the closed events. The mean time constant and relative area for each of the distributions are as follows: 0.55 ms (0.34), 3.3 ms (0.31), 14 ms (0.21), 75 ms (0.08), 606 ms (0.04), and 4,880 ms (0.02).

Dose–Response Curve of Single-channel Currents to $[H^+]_o$

The percentage of time the channel spends in the open state increases with $[H^+]_o$. Fig. 8 plots this relationship for data obtained from patches activated with increasing concentrations of $[H^+]_o$. For each pH_o, the mean P_o was calculated from at least 80,000 open and closed events. For some of the points in Fig. 8, data from three to five patches were combined to have sufficient number of events for the analysis because in these experiments patches were perfused for only 10 s with each solution.

We removed from the analysis the long quiescent periods (≥2,000 ms). This long closures were infrequent but were seen at all pH_o. Its inclusion in the analysis would have introduced a large variability in the P_o among patches activated by the same pH_o because not all patches examined contained these events (10–20 events out of 20,000). If present, the average P_o would be markedly decreased.

The line in Fig. 8 represents the fit of the data to the Hill equation: $P_o = P_{oMax}/(EC_{50}{}^N/[H^+]_o{}^N + 1)$, where P_{oMax} is 0.8, $[H^+]_o$ is the concentration of external protons in micromolars, EC_{50} is the apparent concentration of protons that produces 50% of the maximal activation, and N is the Hill coefficient. The values of the apparent EC_{50} and N obtained from the fitting were 16 ± 4 μM (pH_o = 4.8 ± 0.25, and 2.7 ± 0.3, respectively.

Stability of Channel Kinetics and Modes of Activity

Inspection of single-channel records reveals that the kinetics are not stationary. Channels exhibit sudden changes in P_o and in kinetics. To test for stability of the data and possible kinetic modes, we calculated the mean P_o averaged over 5-s intervals and plotted it versus time. Fig. 9 shows such plots for pH_o 6.0, 5.0, and 4.0. As indicated before, P_o increases with increasing $[H^+]_o$; however, channel activity fluctuates between periods with openings and periods of quiescence, a characteristic that was consistently seen at all pH_o.

Visual inspection of the records and correlation with the P_o stability plots makes evident the presence of distinct modes of activity, which differ in kinetics and P_o. By using P_o as the criterion to classify modes of activity, at least three modes were readily recognized: mode 1 ($P_o < 0.10$), mode 2 ($P_o = 0.5 \pm 0.05$), and mode 3 ($P_o > 0.9 \pm 0.05$; Fig. 10). In mode 1, the channel oscillates rapidly between open and closed states producing a flicker appearance. Mode 2 exhibits high P_o and contains long open events. In contrast, the open events in mode 3 are short, and they are interrupted by closed events of long duration given a low P_o to this mode. Mode 4 (P_o = 0.5–0.8) has less distinct properties, it may constitute a distinct mode or alternatively, it represents transitions of the channel between the other three previous modes.

Single-channel patches were examined with the P_o criterion to detect modes 1, 2, and 3. Data collected from several patches were used to generate the histograms shown in Fig. 11. The distributions of open intervals are described by the sum of two exponentials, whereas the distribution of closed events required two, three, and four exponentials for modes 1, 2, and 3, respectively. Mode 1 contains predominantly intermediate openings, mode 2 contains all the long openings, and mode 3 contains almost exclusively the short openings. The values of the apparent time constants and the

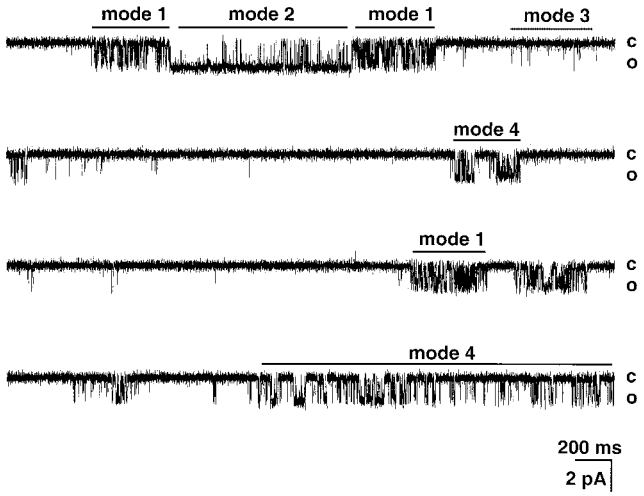

FIGURE 10. Modes of activity of ASIC2-3 channels. The figure shows a continuous record of a single channel activated by pH_o 4.0. The channel exhibits sudden changes in kinetics, which are indicated by bars labeled mode 1, mode 2, mode 3, and mode 4. Holding potential was −80 mV. External and internal solutions contained 150 mM NaCl and 150 KCl, respectively. Closed and open levels are indicated on the right. Current amplitude and time scales are indicated by the bars at the bottom of the record.

percentage of events corresponding to each component are given in the legend of Fig. 11.

Since the criterion for identifying the modes was P_o, all of the long closed events appear in mode 3. These events represent the slowest component (apparent time constant of 5,209 ms) of the histogram of closed events from mode 3. However, the long closed state was not only associated with mode 3, but it could follow or precede any of the other modes, suggesting that this closed state is connected with more than one mode of activity.

The frequency of the activity modes is pH_o dependent. At pH_o 6.0, the channel spends 98 ± 5% of the time in mode 3 and in the long closed state. At pH 5.0, the channel enters all modes and remains: 59 ± 10% in mode 3, 9 ± 3% in mode 2, 7 ± 4% in mode 1, and 25 ± 5% in mode 4. At pH_o 4.0 the channel also enters all modes but spends more time in the high P_o modes: 25 ± 7% in mode 2, 15 ± 15% in mode 3, 10 ± 7% in mode 1, and 50 ± 10% in mode 4 or unclassified.

DISCUSSION

Properties of the Unitary Currents

This is the first report that describes the properties of unitary currents of channels formed by association of ASIC2 and ASIC3 subunits. Our studies revealed that these channels have a slope conductance of 18 pS measured in solutions containing 150 mM Na^+ outside and 150 mM K^+ inside. The permeability for monovalent cations has the sequence $Na^+ > Li^+ > K^+$. We did not detect permeability for Ca^{2+}; on the contrary, millimolar concentrations of Ca^{2+} and other divalent cations block ASIC2-3. These results indicate that opening of ASIC2-3 in vivo produces depolarization of the membrane potential but not activation of Ca^{2+}-mediated second messengers in DRG neurons.

In symmetric solutions, the I-V relationship of unitary currents is linear. Thus, ASIC2-3 is not voltage dependent, a result that agrees with previous observations

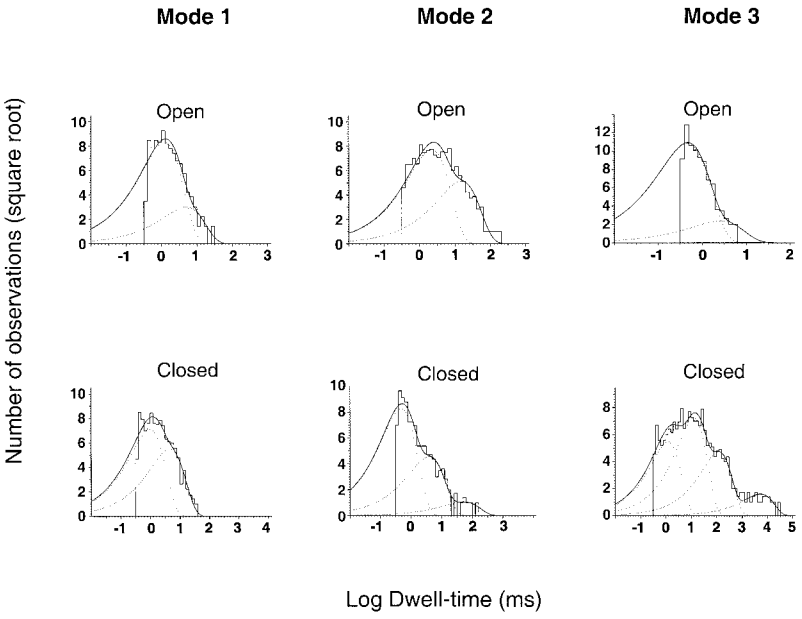

FIGURE 11. Dwell-time histograms of open and closed events corresponding to modes 1, 2, and 3. A long record from a single channel activated by pH_o 4.0, containing 50,000 events was analyzed for moving mean P_o calculated with 100 successive open and close intervals. We assigned to mode 1 segments of the record with P_o 0.5 ± 0.05, to mode 2 $P_o > 0.6$, and to mode 3 $P_o < 0.1$. Events from each mode were pooled and used to construct histograms of open and closed events. (mode 1) The distributions of open times were fitted with the sum of two exponential components with parameters (mean time constant, with the relative area shown in parentheses): 1.24 ms (0.88) and 4.94 ms (0.11). The distributions of closed times were fitted with the sum of two exponential components: 0.98 ms (0.62) and 4.5 ms (0.37). (mode 2) Distributions of open times: 2.24 ms (0.69) and 15.14 ms (0.31). Distributions of closed times were fitted with three exponential components: 0.48 ms (0.76), 3.87 ms (0.23), and 51.2 ms (0.13). (mode 3) Distributions of open times: 0.46 ms (0.94) and 2.0 ms (0.055). Distributions of closed times were fitted with four exponential components: 1.24 ms (0.28), 13 ms (0.48), 121.8 ms (0.21), and 5,209 ms (0.024).

done on whole-cell currents from injected *Xenopus* oocytes (Babinski et al., 2000). We also found that channels with identical conductance and selectivity underlie the fast and sustained components of the macroscopic currents. The only significant difference was a larger number of activated channels in the fast component some of which inactivate, producing a decrease in the magnitude of the current. Another important finding was that the amplitude of the unitary current was not diminished by increasing $[H^+]_o$, indicating that protons do not block the open channel.

Activation by $[H^+]_o$

External protons activate ASIC2-3 in a concentration-dependent manner by increasing the P_o. The relation between P_o and $[H^+]_o$ was described by a slope to the power of 2.7, suggesting that two or more H^+ ions are required for channel opening. Since $[H^+]_o$ increased the number of openings and also the mean channel open time, both cooperativity of H^+ on channel opening and an effect on prolonging the open time, could contribute to the N greater than two.

Inspection of records containing single channels indicates that ASIC2-3 exhibits complex kinetics. Analysis of dwell-time histograms of open and closed events revealed the presence of at least three open and six closed states. In addition, channels exhibit modes of activity that can be classified, on the basis of P_o and kinetics, into four modes; modes 1–3 are distinct, whereas mode 4 could represent sudden shifts between the other three apparent modes of activity.

ASIC2-3 also exhibits an inactivated state that forms the basis of the fast component of the macroscopic current. Inactivation occurs only in a population of channels and it takes place shortly after lowering the pH_o. To reactivate these channels with H^+_o, the pH_o must first return to 7.4.

The mechanism by which the channel enters the different conformations defining each of the modes of activity is unknown. Sudden changes in kinetic states have been observed on other channels such as the glutamate-activated channels (Patlak et al., 1979) and fast chloride channels from rat skeletal muscle (Blatz and Magleby, 1986). Shifts in activity could occur if a channel makes transitions between two or more different groups of open and closed states, with each group having different kinetics. Shifts in activity could also occur if the binding of protons changes one or more rate constants. Indeed $[H^+]_o$ has a clear effect on determining the frequency of the modes. The observation that at pH_o of 6.0, the channel remains mostly in mode 3, whereas at pH_o 4.0, modes 2 and 4 dominate the activity indicates that higher $[H^+]_o$ are required to enter the modes with high P_o. In addition to increasing the frequency of entering those modes, $[H^+]_o$ also increased the duration of the bursts of activity in modes 2 and 4.

Detection of different modes of activity can give information about the underlying molecular mechanism and allow more direct data analysis. A comprehensive model that describes the kinetics of ASIC2-3 should include the various modes of activity and the way they are connected. Although we have not included in this work a quantitative description of the kinetics of ASIC2-3, our more qualitative studies of the single-channel behavior provide a means to distinguish ASIC2-3 from other channels in DRG neurons.

Physiological Significance of Activation by Protons

The question remains whether H^+ ions gate ASIC2-3 or if some other kind of stimulus opens this channel under physiological conditions. Many investigators have reported the presence of various proton-activated currents in DRG neurons (Akaike et al., 1990; Bevan and Yeats, 1991). One type of proton-activated current is also stimulated by capsaicin and has a high permeability for Ca^{2+}; undoubtedly, this type is mediated by the vallinoid receptor 1. Instead, the other component shares many properties with ASIC-mediated currents: it is insensitive to capsaicin, impermeable to Ca^{2+} (Zeilhofer et al., 1997), and persists after inactivation of the vallinoid receptor (Caterina et al., 2000). The lack of inactivation of ASIC2-3 in the presence of high $[H^+]_o$ and the graded response to $[H^+]_o$ makes this channel a good candidate to sense both sustained changes in pH_o and also to detect gradual changes in external acidification independent of the starting pH_o. This is in contrast with ASIC1, which rapidly inactivates in the presence of external protons, and requires a pH_o close to 7.4 to be reactivated (Waldmann et al., 1997a).

The recent finding that knockout of the ASIC2 gene in mice reduces touch (Price et al., 2000) suggests that ASIC2 may participate in the perception of mechanical stimulus. However, it has yet to be established whether ASIC or the degenerins are the direct receptors for mechanical stimuli or whether they have other roles in neurons that respond to mechanical stimulation. Alternatively, ASIC2-3 could be activated by several types of stimuli, including mechanical and acidification of the extracellular medium. Indeed, it has been shown that low pH_o induces a significant and lasting decrease of the mechanical thresholds in C-fibers that originate from a set of small root ganglion cells (Steen et al., 1992). The notion that a channel can be activated by more than one stimulus is not unique to ASIC. In DRG neurons, the vallinoid receptor serves as a polymodal signal detector; it is gated by vallinoid compounds, heat, and protons (Tominaga et al., 1998).

Although this work does not solve the above questions, the single-channel properties we have described

here need to be consistent with the functional role(s) ultimately assigned to ASIC in the peripheral nervous system.

This work was supported by the National Institutes of Health grant K01HL56163 to C. Canessa. The work was done under the tenure of an American Heart Association Postdoctoral Fellowship to P. Zhang.

Submitted: 5 December 2000
Revised: 30 April 2001
Accepted: 1 May 2001

REFERENCES

Akaike, N., O.A. Krishtal, and T. Maruyama. 1990. Proton-induced sodium current in frog isolated dorsal root ganglion cells. *J. Neurophysiol.* 63:805–813.

Akopian, A.N., C.C. Chen, Y. Ding, P. Cesare, and J.N. Wood. 2000. A new member of the acid-sensing ion channel family. *Neuroreport.* 11:2217–2222.

Babinski, K., S. Catarsi, G. Biagini, and P. Séguéla. 2000. Mammalian ASIC2a and ASIC3 subunits co-assemble into heteromeric proton-gated channels sensitive to Gd^{3+}. *J. Biol. Chem.* 275:28519–28525.

Bevan, S., and J. Yeats. 1991. Protons activate a cation conductance in a sub-population of rat dorsal root ganglion neurons. *J. Physiol.* 433:145–161.

Blatz, A.L., and K.L. Magleby. 1986. Quantitative description of three modes of activity of fast chloride channels from rat skeletal muscle. *J. Physiol.* 378:141–174.

Caterina M.J., A. Leffler, A.B. Malmberg, W.J. Martin, J. Trafton, K.R. Petersen-Zeitz, M. Koltzenburg, A.I. Basbaum, and D. Julius. 2000. Impaired nociception and pain sensation in mice lacking the capsaicin receptor. *Science.* 288:306–313.

Chen, C.C., S. England, A.N. Akopian, and J.N. Wood. 1998. A sensory neuron-specific, proton-gated ion channel *Proc. Natl. Acad. Sci. USA.* 95:10240–10245.

Corey, D.P., and J. Garcia-Añoveros. 1996. Mechanosensation and the DEG/ENaC ion channels. *Science.* 273: 323–324.

Driscoll, M., and M. Chalfie. 1991. The mec-4 gene is a member of a family of *Caenorhabditis elegans* genes that can mutate to induce neuronal degeneration. *Nature.* 349:588–593.

Fyfe, G.K., A. Quinn, and C. Canessa. 1998. Structure and function of the Mec-ENaC family of ion channels. *Semin. Nephrol.* 18:138–151.

Garcia-Añoveros, J., B. Derfler, J. Neville-Golden, B.T. Hyman, and D.P. Corey. 1997. BNaC1 and BNaC2 constitute a new family of human neuronal sodium channels related to degenerins and epithelial sodium channels. *Proc. Natl. Acad. Sci. USA.* 94:1459–1464.

Gründer, S., H.S. Geissler, E.L. Bassler, and J.P. Ruppersberg. 2000. A new member of acid-sensing ion channels from pituitary gland. *Neuroreport.* 11:1607–1611.

Huang, M., and M. Chalfie. 1994. Gene interactions affecting mechanosensory transduction in *Caenorhabditis elegans. Nature.* 367:467–470.

Lingueglia, E., J.R. De Weille, F. Bassilana, C. Heurteaux, H. Sakai, R. Waldmann, and M. Lazdunski. 1997. A modulatory subunit of acid sensing ion channels in brain and dorsal root ganglion cells. *J. Biol. Chem.* 272:29778–29783.

Patlak, J.B., K.A.F. Gration, and P.N.R. Usherwood. 1979. Single glutamate-activated channels in locust muscle. *Nature.* 278:643–645.

Price, M.P., P.M. Snyder, and M.J. Welsh. 1996. Cloning and expression of a novel human brain Na^+ channel. *J. Biol. Chem.* 271: 7879–7882.

Price, M.P., G.R. Lewin, S.L. Mcllwrath, C. Cheng, J. Xie, P.A. Heppenstall, C.L. Stucky, A.G. Mannsfeldt, T.J. Brennan, H.A. Drummond, et al. 2000. The mammalian sodium channel BNC1 is required for normal touch sensation. *Nature.* 407:1007–1011.

Steen, K.H., P.W. Reeh, F. Anton, and H.O. Handwerker. 1992. Protons selectively induce lasting excitation and sensitization to mechanical stimulation of nociceptors in rat skin, *in vivo. J. Neurosci.* 12:86–95.

Tominaga, M., M.J. Caterina, A.B. Malmberg, T.A. Rosen, H. Gilbert, K. Skinner, B.E. Raumann, A.I. Basbaum, and D. Julius. 1998. The cloned capsaicin receptor integrates multiple pain-producing stimuli. *Neuron.* 3:531–543.

Waldmann, R., G. Champigny, F. Bassilana, C. Heurteux, and M. Lazdunski. 1997a. A proton-gated cation channel involved in acid-sensing. *Nature.* 389:173–177.

Waldmann, R., F. Bassilana, J. deWeille, G. Champigny, C. Heurteux, and M. Lazdunski. 1997b. Molecular cloning of a non-inactivating proton-gated Na^+ channel specific for sensory neurons. *J. Biol. Chem.* 272:20975–20978.

Waldmann, R., G. Champigny, E. Lingueglia, J.R. De Weille, C. Heurteaux, and M. Lazdunski. 1999. $H(^+)$-gated cation channels. *Ann. NY Acad. Sci.* 868:67–76.

Zeilhofer, H.U., M. Kress, and D. Swandulla. 1997. Fractional Ca^{2+} currents through capsaicin- and proton-activated ion channels in rat dorsal root ganglion neurons. *J. Physiol.* 503:67–78.